Supplementary

Microwave Sintering of Ti6Al4V: Optimization of Processing Parameters for Maximal Tensile Strength and Minimal Pore Size

Dilpreet Singh [1], Abhishek Rana [1], Pawan Sharma [2], Pulak Mohan Pandey [2] and Dinesh Kalyanasundaram [1,3,*]

1 Centre for Biomedical Engineering, Indian Institute of Technology Delhi, New Delhi-110016, India; dilpreet.iitdelhi@gmail.com (D.S.); Abhishek.rana130@gmail.com (A.R.)
2 Department of Mechanical Engineering, Indian Institute of Technology Delhi, New Delhi -110016, India; scholarpawansharma@gmail.com (P.S.); pmpandey@mech.iitd.ac.in (P.M.P.)
3 Department of Biomedical Engineering, All India Institute of Medical Sciences, New Delhi -110016, India
* Correspondence: dineshk.iitdelhi@gmail.com or dineshk@cbme.iitd.ac.in; Tel.: +91-11-26597344

S1. Particle Size Distribution of the Ti6Al4V Powder.

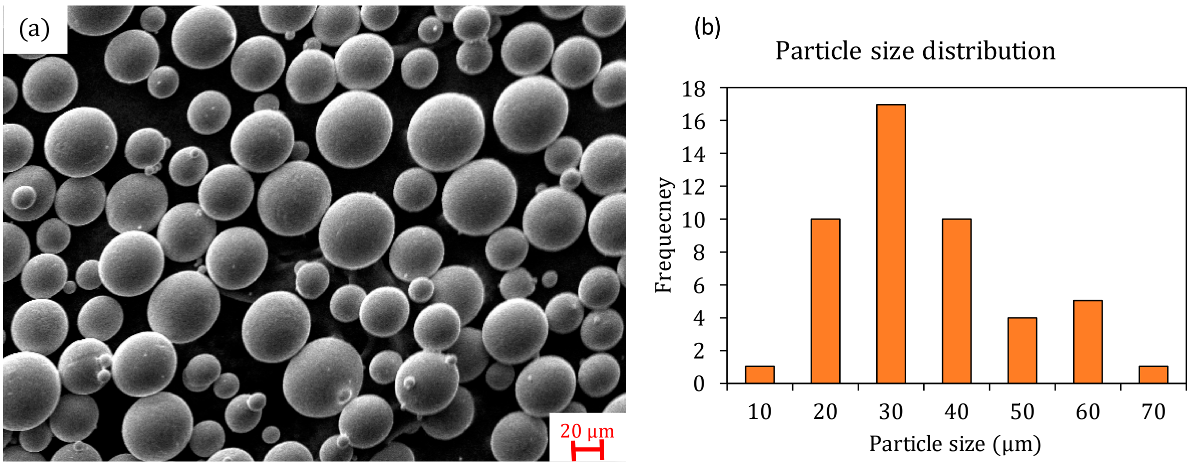

Figure S1. (**a**) Scanning Electron Microscopy (SEM) image of raw spherical powder particles; (**b**) particle size distribution of the powder particles.

The size of the particles of the alloy powder ranged between 10 µm to 70 µm, as seen in Figure S1. Image J®, a free software, was used for the analysis of the particle size distribution.

S2. Microwave Sintering.

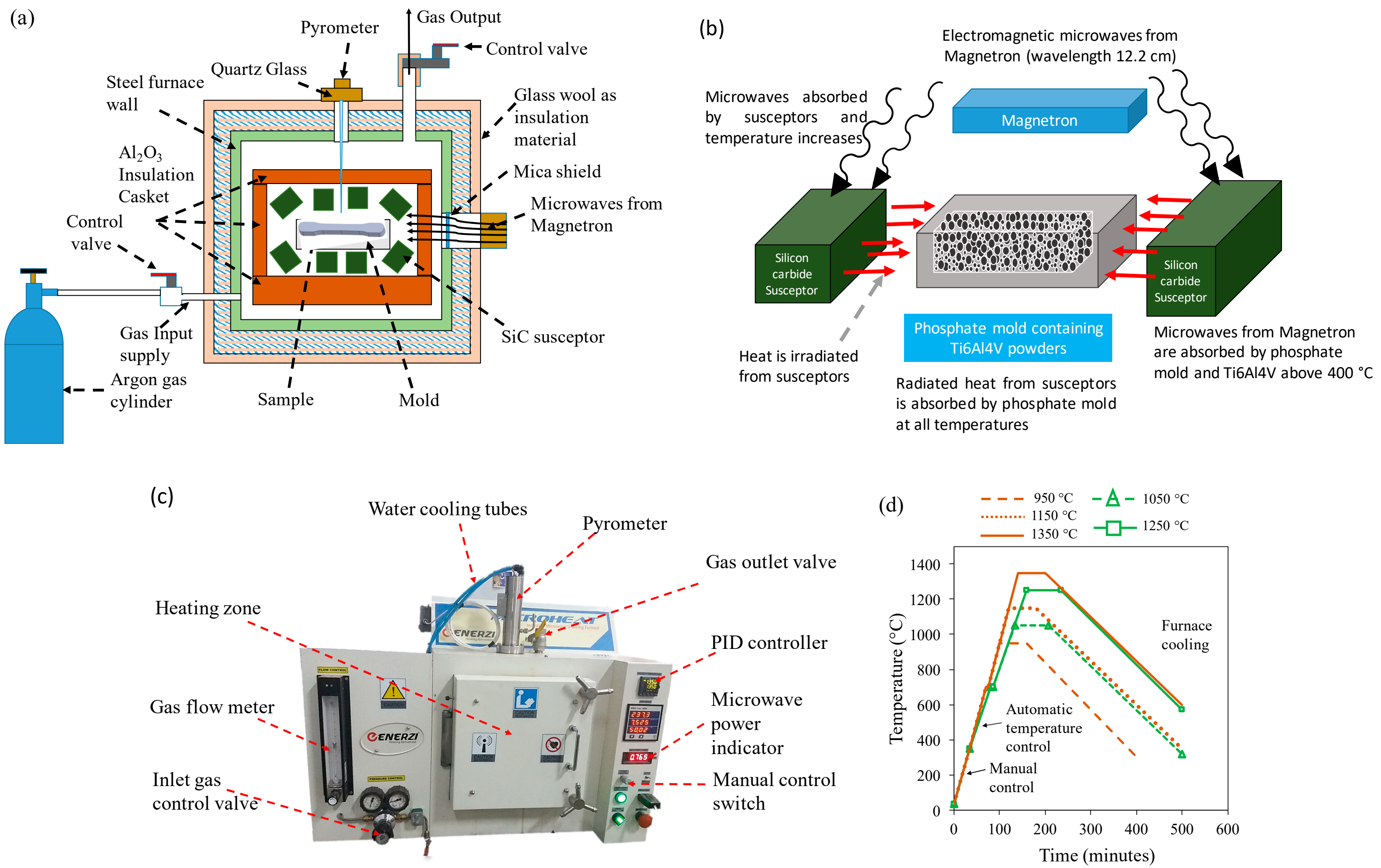

Figure S2. (**a**) Schematic of microwave sintering equipment; (**b**) mechanism of heat transfer; (**c**) actual sintering equipment; and PID stands for Proportional Integral Derivative; (**d**) sintering cycles.

S3. Tensile Testing of Sintered Samples.

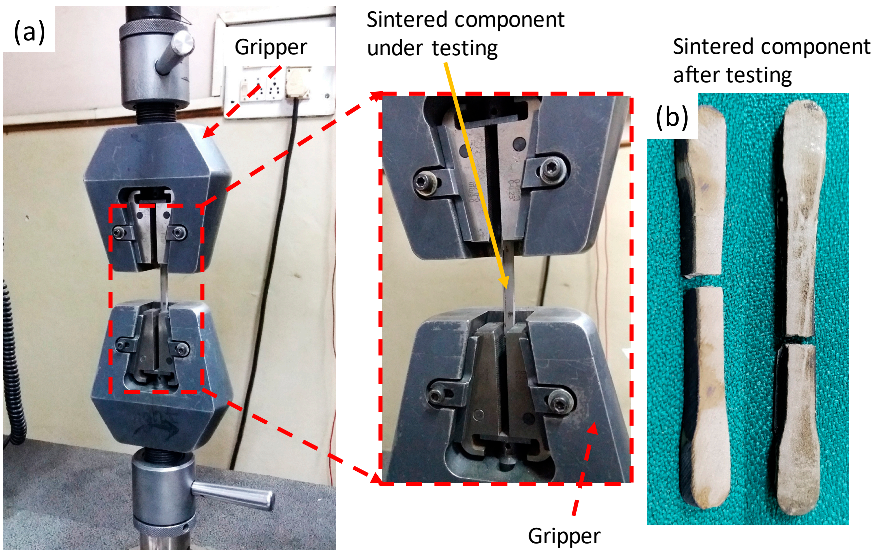

Figure S3. (**a**) Loading of components for tensile testing; (**b**) sintered components post testing.

S4. Micro-Computed Tomography of the Ti6Al4V Samples.

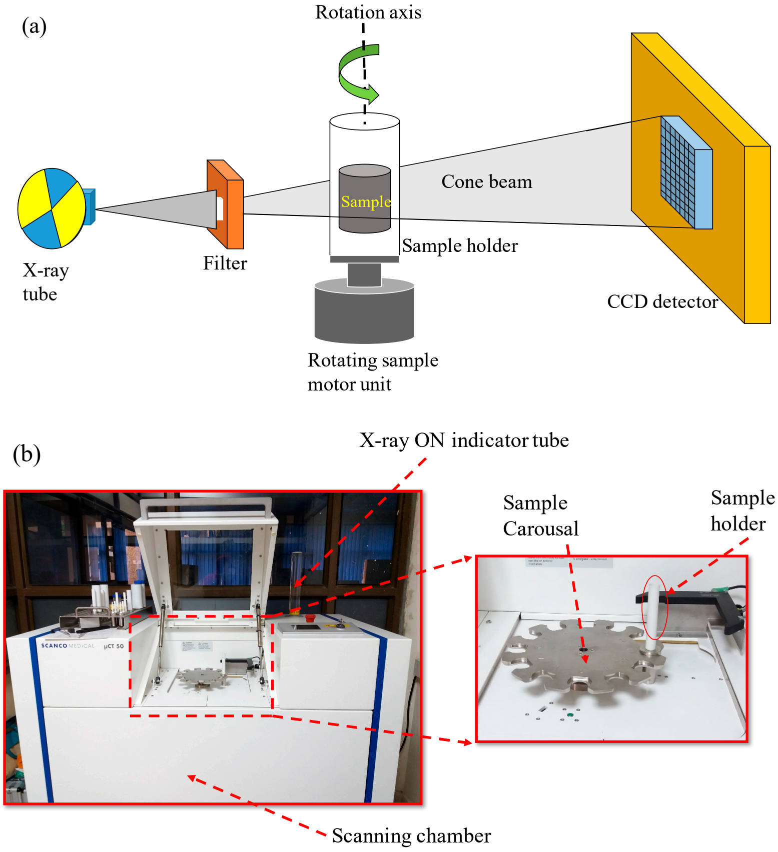

Figure S4. (**a**) Schematic for the micro-Computed Tomography scanning arrangement; (**b**) picture of the micro-Computed Tomography equipment.

S5. X-ray Diffractometry Analysis.

The X-ray diffractometry (XRD) analysis was performed for the raw titanium alloy powder and the microwave sintered components. The peaks corresponding to the titanium oxide phase were formed during the microwave sintering process. All the sintering experiments were performed in the β–phase region (>853 °C). The XRD peaks confirm the formation of the β–phase in the sintered components. Furthermore, the peaks related to the presence of aluminum oxide and vanadium oxides were also confirmed in the XRD analysis. Figure S5 shows the XRD spectrum for the bare titanium alloy and the components sintered at *St* of 950 °C, 1150 °C, and 1350 °C, with a *Hr* of 10 °C/minute and *Ht* of 60 minutes. It has been also confirmed from the peaks that the nitrides were also formed during the sintering. This presence of nitride phase may have occurred due to the presence of impurities present in the alumina board, which was used as the insulation material for the sintering of the titanium alloy inside the microwave furnace. The formation of titanium nitride phase due to the impurities and heating at the higher temperature was also confirmed in the literature [1] . The XRD analysis of the raw titanium alloy confirmed the presence of a TiO_2 layer, formed over the powder particle surface. The presence of a oxygen deficient phase, such as Ti_2O_3 and Ti_3O_5, during the microwave sintering of the titanium was also confirmed in the literature [2]. The Joint committee on powder diffraction standards (JCPDS) database was used for identifying the peaks with the following JCPDS card numbers: JCPDS 84 1750, 10 0063, 77 1392, 71 0290, 73 2294, 82 1137, 02 1159, 73 1570, 44 1294, 73 0959, 84 0319, 73 1774, 01 072 1807, 01 073 1782.

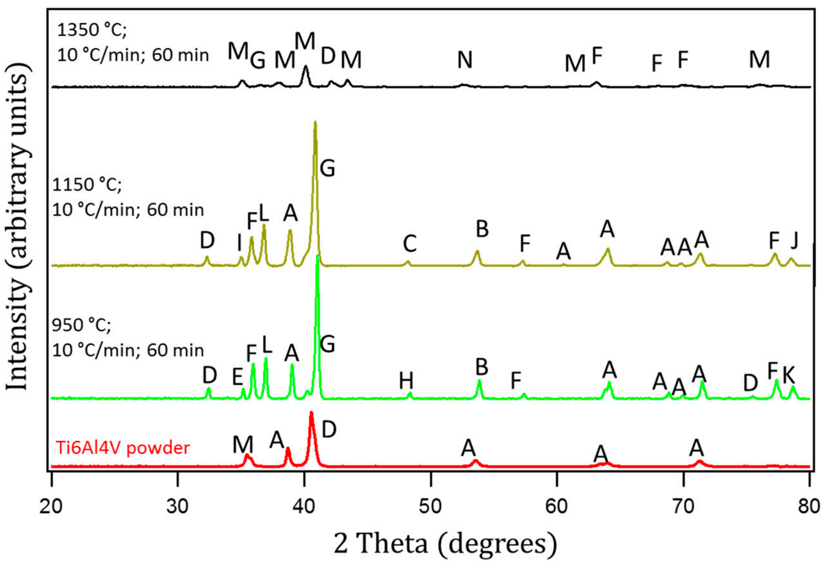

Notations	Compound
A	TiO_2
B	Ti_2O_3
C	Ti_4O_7
D	VO_2
E	Al_2O_3
F	Ti_3O_5
G	TiN
H	TiO_5
I	Ti
J	Ti_2N
k	V_2O_3
L	$TiO_{0.716}$
M	Ti_6O
N	$TiO_{1.95}$

Figure S5. X-ray diffractometry analysis for the titanium alloy sintered at *St* —950 °C, 1150 °C, and 1350 °C, and *Hr*—10 °C/minute and *Ht*—60 minute, along with the raw titanium alloy powder.

Reference

1. Luo, S.D.; Qian, M. Microwave processing of titanium and titanium alloys for structural, biomedical and shape memory applications: Current status and challenges. *Mater. Manuf. Processes* **2018**, *33*, 35–49. doi:10.1080/10426914.2016.1257800.
2. Cheng, J.P.; Agrawal, D.K.; Komarneni, S.; Mathis, M.; Roy, R. Microwave processing of WC-Co composities and ferroic titanates. *Mater. Res. Innovations* **1997**, *1*, 44–52. doi:10.1007/s100190050017.